Journal of Materials Chemistry A

RSC Publishing

PAPER

View Article Online
View Journal | View Issue



Cite this: J. Mater. Chem. A, 2013, 1, 8379

# Graphene–ionic liquid electrolytes for dye sensitised solar cells

Lorcan J. Brennan, Sebastian T. Barwich, Amro Satti, Adeline Faure and Yurii K. Gun'ko*

Received 23rd April 2013
Accepted 2nd May 2013

DOI: 10.1039/c3ta11609c

www.rsc.org/MaterialsA

In this work two dimensional graphene flakes were used to prepare new electrolytes for dye sensitized solar cells (DSSCs). Small amounts (up to 3 wt%) of graphene nanoflakes were suspended into the ionic liquid (IL) 1-propyl-3-methyl imidazolium iodide (PMII) to produce new electrolytes. The use of these electrolytes in DSSCs resulted in more than twenty five times improvement of the solar cell efficiency. The increase in efficiency can be attributed to two primary reasons. Graphene can act as an efficient charge transfer agent in the viscous IL and also as a catalyst for the electrochemical reduction of $I_3^-$ in the electrolyte layer. In addition interactions between the graphene and the IL system lead to the formation of self-organised assemblies or networks. These factors not only provide an efficient electron transfer network through the electrolyte but also allow for the formation of quasi-solid electrolytes, at higher graphene concentrations. These electrolytes may find applications in advanced DSSC architectures, where a quasi-solid based system could eliminate problems associated with electrolyte leakage and solvent related degradation of materials.

## 1 Introduction

With the decline in the earth's natural energy resources and the increasing cost associated with the supply of fossil fuel based energy much research has focused on the generation of electricity from alternative 'green' energy sources. Such sources include wind, hydro and solar energies. Of all these types, solar energy provides by far the most abundant and practical energy source which may have the potential to reduce the need for fossil fuel associated energy. Silicon based solar technologies currently dominate the market. However, the purification and fabrication process which requires high temperature and high vacuum conditions as well as many lithographic steps is quite expensive. This is a barrier which impedes large scale, affordable electricity generation from sunlight. In light of this there is great demand for new and affordable solar cells which can generate electricity from light.

The dye-sensitized solar cell (DSSC) offers a potentially cheap and sustainable solution to this problem. The DSSC was developed by Gratzel and O'Regan in 1991.[1] Since that time the research into DSSCs has progressed rapidly, offering cheaper and easier solutions than conventional Si cells.[2,3] Despite the power conversion efficiency of the DSSC being lower than Si, DSSCs offer some key advantages to Si based technologies.[4] DSSCs can operate under diffuse lighting conditions and can thus generate electricity indoors or on a cloudy day, these cells also show increased efficiency with increasing temperature which is unlike semiconducting Si based devices.

The electrolyte is one of the key components of DSSCs. The function of the electrolyte is to transfer charge from the counter electrode (CE) to the dye which is anchored onto the mesoporous $TiO_2$ charge collection layer. In order to work effectively the electrolyte must fulfil some key characteristics including thermal stability, high diffusion coefficient and suitable viscosity which will allow for ease of sealing without impeding the transfer of charge.[5,6] Traditional DSSC technology has focused on the use of organic solvent based electrolytes which cause a number of problems during manufacturing. These problems include leakage of the electrolyte, degradation of the polymer seal and evaporation of the solvent which all limit cell lifetime and hence long-term applications. These disadvantages are serious obstacles that face the successful commercialization of DSSC technology, in particular the large scale development of flexible modules.

Ionic liquids (ILs) have received much attention in recent years as a potential substitute to the organic solvent based electrolytes currently employed in DSSCs. Room temperature ILs are molten salts with characteristics highly suitable for DSSC electrolytes. Some of these characteristics include tuneable viscosity, non-volatility, ionic conductivity, excellent thermal stability, a broad electrochemical potential window and negligible vapour pressure.[7–9] Unfortunately the conversion efficiencies achieved with ILs at full air mass (AM 1.5) do not match those of solvent electrolytes. This is due to the fact that the diffusion coefficient of the redox pair in the viscous molten salt is generally 1–2 orders of magnitude lower than that of ionic

School of Chemistry and CRANN, Trinity College Dublin, Dublin 2, Ireland. E-mail: igounko@tcd.ie; Tel: +353 1 8963543

diffusion in an organic solvent.[10] Several approaches have been investigated towards designing an IL electrolyte which retains the characteristics of the IL but yet achieves conversion efficiency closer to that of the solvent based electrolytes. Such approaches have included the incorporation of various nanocomponents,[11–13] the use of polymer IL composites,[14,15] organic/inorganic gel electrolytes,[13] hole conducting materials[16] and carbon nanomaterials.[17]

Graphene is the basic building block for graphitic materials of all other dimensions. Graphene, a two-dimensional carbon sheet, consists of $sp^2$ hybridised carbon atoms which are arranged into a honeycomb lattice. The current interest in graphene is attributed to its excellent electronic and thermal conductivity, transparency, flexibility and remarkable mechanical and chemical stability.[18] All of these properties make graphene an excellent prospective material for the future with applications in technologies such as transparent conducting flexible materials,[19–21] ultra-strong and stable graphene polymer composites[22–25] and photovoltaic cells.[19,26–28]

Previously we have demonstrated that very viscous quasi-solid state electrolytes can be prepared by the incorporation of graphene or carbon nanotubes into ionic liquids.[17] Using these new electrolytes, significant increases in light conversion efficiencies of DSSCs have been achieved. In the present work the IL 1-propyl-3-methyl imidazolium iodide (PMII) with addition of small amounts of dispersed graphene sheets was employed as a DSSC electrolyte. Work by Fukushima *et al.* has shown that carbon nanomaterials can be readily exfoliated in imidazolium based ILs due to the π–π interaction that exists between the imidazolium ring and the extended delocalised ring structure of the graphene.[9,29] Graphene was expected to serve as an extended electron transfer surface (EETS) in the electrolyte which can provide an augmented electron transfer from the CE to the PMII,[17] thus resulting in a reduced charge diffusion length. Graphene has been shown to be electro-catalytically active towards reduction of $I_3^-$,[30] hence it was expected that graphene nanosheets suspended in the IL medium would act as an electro-catalyst for the reduction of $I_3^-$ in the electrolyte.

## 2 Experimental

### 2.1 Materials

Graphite powder was obtained from Alfa Aesar; 1-propyl-3-methyl imidazolium iodide (PMII) was supplied by Iolitec and used as received. $TiO_2$ working electrodes and Pt counter electrodes were fabricated on FTO glass (12 Ω $\square^{-1}$, Sigma Aldrich, NSG TEC12). $TiO_2$ powder (P25) was received from Degussa. Sensitizing ruthenium dye ($RuLL'(NCS)_2$ (L = 2,2′-bipyridyl-4,4′-dicarboxylic acid; L′ = 4,4′-dinonyl-2,2′-bipyridine) (Z907)) was purchased from Dyesol limited. Chloroform (HPLC grade) was purchased from Fisher scientific. *tert*-Butanol, acetonitrile, tetraethylammonium tetrafluoroborate and chloroplatinic acid were purchased from Sigma-Aldrich. All materials were used as received unless otherwise stated.

$TiO_2$ electrodes were prepared on FTO coated glass substrates. Glass substrates were cleaned in a detergent solution with ultrasonication for 15 minutes followed by sonication in ethanol (10 min) and acetone (10 min). A bulk $TiO_2$ layer was applied to the FTO coated glass from a 40 mM aqueous $TiCl_4$ solution. FTO glass plates were submerged in the $TiCl_4$ solution at 70 °C for 30 minutes. Once removed, the glass was washed with water and alcohol. In order to form the mesoporous electrode $TiO_2$ paste was applied to FTO coated substrates using the screen printing method. $TiO_2$ pastes were fabricated according to the procedure outlined by Ito *et al.*[31] Electrodes were produced by several coatings of the prefabricated paste onto FTO substrates until a thickness of 12–13 μm was achieved. Following this, 2 layers of light scattering $TiO_2$ (150–200 nm) (Dyesol WERO-2) were deposited. $TiO_2$ working electrodes were treated to a sintering profile which consisted of a drying period at 125 °C for 6 minutes, ramping to 350 °C and holding for 15 minutes, ramping to 450 °C and holding for 15 minutes and finally sintering at 500 °C for 15 minutes. A ramping rate of 8 °C $min^{-1}$ was used for all ramping steps. Once cooled the electrodes were immersed into a 40 mM aqueous $TiCl_4$ solution and heated to 70 °C for 30 minutes. Upon removal from the bath electrodes were cleaned with water and alcohol and treated to a second sintering step at 500 °C for 30 minutes. The electrodes were allowed to cool to 80 °C and were then immersed into a solution of Z907 (0.3 mM) in a mixture of acetonitrile and *tert*-butanol (vol ratio 1 : 1). $TiO_2$ electrodes were allowed to soak in the bath for periods of approximately 16 hours. The final $TiO_2$ thickness was 15.5–17 μm (SEM). Pt counter electrodes were prepared by first drilling a small hole (3 mm) through the FTO coated glass. A cleaning procedure in Millipore water was followed by cleaning with 1 M aqueous HCl and finally sonication in acetone for 10 minutes. Residual organics were removed by heating the glass to 400 °C for 15 minutes. Pt was deposited by drop-casting an aqueous solution of chloroplatinic acid (4.5 mM) onto the FTO surface, followed by a heat treatment at 400 °C for 15 minutes.

The DSSCs were sealed using a Surlyn spacer (60 m) and the composite electrolyte was introduced into the cell under vacuum and sealed with Surlyn and a small piece of glass.

### 2.2 Characterisation techniques and instrumentation

The Raman scattering measurements were performed using a Jobin Yvon Labram HR equipped with a CCD detector and a 100× long working distance lens. The He–Ne laser with an excitation wavelength of 535 nm and a maximum power of 12 mW was used with a diffraction grating with 600 lines per mm. The laser was used at 10% of maximum power and acquisition times and cycles were set to obtain a high signal to noise ratio of all peaks of interest (>10 : 1). Ten spectra were taken per sample to allow an average measurement of the sample to be obtained and to increase the signal to noise ratio further. The spectrometer was calibrated using a Si sample before use and the system has a quoted resolution of 0.3 $cm^{-1}$ when properly calibrated.

The ultrasonic bath employed was a Grant XB6 which operated at 50–60 Hz. Centrifugation was carried out using a Hettich Universal 32. UV-vis absorption spectra were recorded at room temperature using a Shimadzu UV2101 PC UV-vis scanning spectrometer. The samples were examined in a 1 cm quartz cell.

 

TEM images were taken using a Joel 2100 electron microscope. The TEM operated at a beam voltage of 200 kV. The samples being analysed were diluted by a factor of ten and drop casted onto holey carbon grids at ambient temperature and allowed to dry.

Cyclic voltammetry was performed on a computer controlled μ-autolab type III potentiostat controlled by autolab 1.4 software.

*I–V* measurements were performed using a digital source meter (Keithley 2400) and a full spectrum solar simulator (Newport 96000), fitted with a Xe arc discharge lamp operated at 150 W which was equipped with a 1.5D air mass filter and calibrated with a silicon-based reference cell before testing. All cells were tested at 1000 W $m^{-2}$, with an active area of 0.17 $cm^{-2}$, defined by a mask.

## 3 Results and discussion

### 3.1 Graphene preparation and characterisation

Exfoliation of the graphite to prepare graphene followed the procedure similar to that outlined by O'Neill *et al.*[32] Briefly the graphite was dispersed in chloroform at a concentration of 1 mg $ml^{-1}$. The solution was then placed in an ultrasonic bath and ultrasonicated for a period of ~100 hours to ensure maximum exfoliation of the graphite. After this process the solution was centrifuged at 500 RPM for 1 hour. Following this the supernatant was decanted off leaving the unexfoliated graphite in precipitate. The resulting dark coloured suspension was deposited onto holey carbon grids for TEM analysis (see below). The graphene solutions were vacuum filtered onto Durapore (0.2 μm) membranes. The graphene dispersions were then added to PMII at various concentrations ranging from 0.125 wt% to 3 wt% and the residual chloroform was removed with vacuum assisted heating in a Schlenk vessel. The resulting PMII graphene composites were utilized as electrolytes in DSSCs.

The formation of the resulting graphene was confirmed by both TEM and Raman spectroscopy.

Raman spectroscopy (Fig. 1) clearly demonstrated that solvent exfoliation of graphite resulted in the production of multi-layered graphene. The Raman spectra of graphitic materials are composed of 3 distinct peaks. The D peak located at ~1350 $cm^{-1}$ gives an insight into the level of disorder in the sample. The G peak located at ~1580 $cm^{-1}$ and the 2D located at ~2700 $cm^{-1}$ are always present in graphitic samples. The shape of the peaks and the relationship between there intensities can be used very effectively to gain an insight into the level of exfoliation in a graphitic sample.[33]

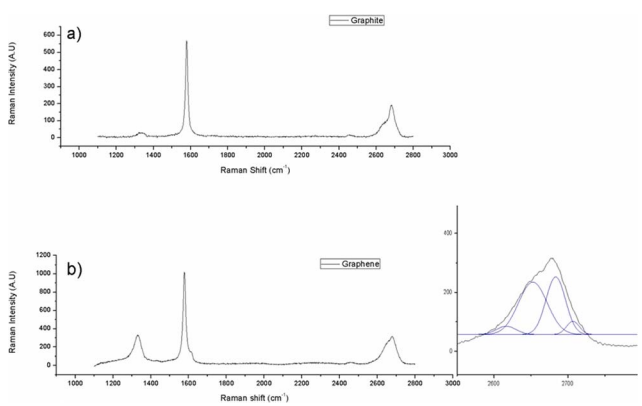


**Fig. 1** Comparative Raman spectra recorded for graphite and graphene film prepared through vacuum filtration of exfoliated graphene solution. The inset shows the four component peaks of the 2D graphene peak.

The Raman spectra obtained for a graphite film prepared from chloroform without any ultra-sonication are shown in Fig. 1a. A small D band can be observed at ~1350 $cm^{-1}$, this peak is an indication of defects in the sample most likely caused by the edges of the graphite flakes present.

The relationship in intensity between the G and 2D peaks (4 : 1) clearly shows that the sample is composed of bulk graphite. This is further backed up by the shape of the 2D peak where the shoulder located at ~2650 $cm^{-1}$ is indicative of graphite. Fig. 1b displays the Raman spectra recorded for the film prepared after a 100 hour sonication in chloroform. Ten individual scans were taken of this film and the data obtained were averaged and presented as the Raman spectra shown in the figure. Clear differences in the size and shape of the graphitic peaks show the presence of exfoliated graphite. Monolayer graphene cannot be expected to be observed using this sample preparation. The filtration process will inevitably cause exfoliated flakes to restack on top of each other, however it is expected that the flakes will not aggregate in the same orientation as that found in bulk graphite. The Raman spectra recorded show an intense D peak which can be attributed to the larger number of flake edges present in the exfoliated sample.[34] The change in shape of the 2D peak is the clearest indication of exfoliated graphite. The broad shoulder observed in bulk graphite is no longer present and this is consistent with what is expected from a graphene film which has not aggregated back into the bulk form.[35] The 2D peak of the graphene film is composed of 4 distinct peaks $2D_{1B}$, $2D_{1A}$, $2D_{2A}$, and $2D_{2B}$ which give an indication into the extent of exfoliation in the sample. This feature is not observed in our graphite 2D band, which consists solely of $D_1$ and $D_2$ component peaks.[33]

TEM analysis confirmed the presence of highly exfoliated multilayered graphene (Fig. 2). Images B, C and D show the presence of graphene layers. The folding edge of the sheet in image B is a common feature associated with monolayer graphene. Graphene layers can be observed in images B, C and D and show the extent of exfoliation when compared to the bulk graphite (A).

### 3.2 Electrochemical analysis of graphene–ionic liquid electrolytes

In order to gain an insight into the effect of graphene on the redox activity of the ionic liquid we carried out cyclic voltammetry (CV) studies. Fig. 3 shows the CV curves obtained for the $I^-/I_3^-$ system with and without the presence of varying concentrations of graphene. CV scans were studied over a potential window of −0.4 to 1.18 V *vs.* a saturated (KCl) calomel reference electrode.

The cyclic voltammogram of the $I^-/I_3^-$ redox couple consists of a pair of redox waves, as can be seen in Fig. 3.

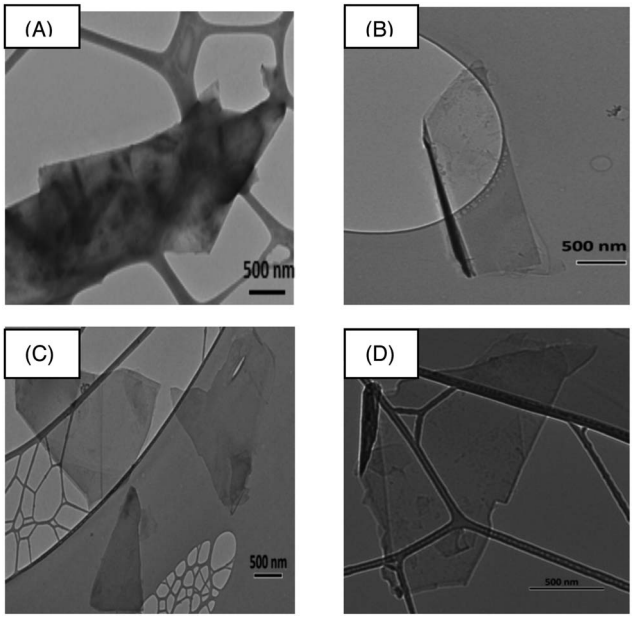


**Fig. 2** Transmission electron microscope images of (A) graphite and (B–D) graphene exfoliated in chloroform at a concentration of 1 mg ml$^{-1}$. Scale bar reads 500 nm for all of the images.

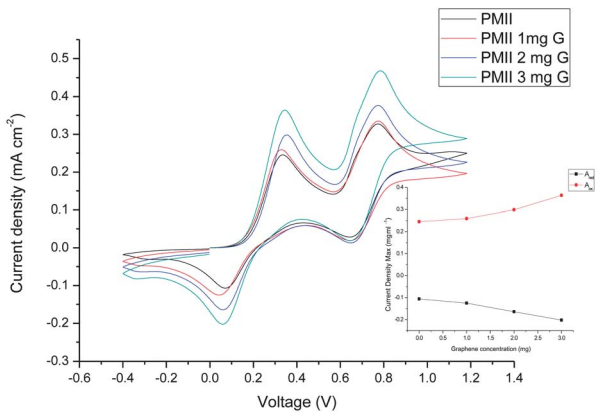


**Fig. 3** Cyclic voltammograms recorded for PMII (black line) and PMII with increasing graphene concentration (red-blue-green). CV curves were obtained at a scan rate of 75 mV s$^{-1}$. The electrochemical cell consisted of a gold working electrode (3 mm$^2$) and a Pt wire counter electrode. A saturated calomel (KCl) reference electrode was employed for all scans. The stock electrolyte consisted of a 0.1 M tetraethylammonium tetrafluoroborate (supporting electrolyte) and 1.0 mM PMII in acetonitrile. Graphene was added incrementally from 1 mg to 3 mg.

The first redox wave, which is located at lower potential, holds most interest for studying electron transfer mechanisms in DSSCs, as it corresponds to the oxidation (anodic peak) and reduction (cathodic peak) of $I_3^-$ *via* the following electron transfer reaction:

$$I_3^- + 2e^- \leftrightarrow 3I^- \quad (A)$$

The second redox peak (higher potential) is attributed to the electron transfer mechanism below:

$$3I_2 + 2e^- \leftrightarrow 2I_3^- \quad (B)$$

One proposed mechanism for our observed increase in solar cell efficiency is the development of an extended electron transfer surface which allows for tri-iodide reduction to occur on graphene sheets which are located in the electrolyte. We believe that the presence of graphene reduces the diffusion length of the species in the viscous ionic liquid and thus results in an increase in solar cell efficiency. The CV results show a clear increase in the current–response obtained in the presence of graphene located in the electrolyte. Examination of the first redox wave (A) demonstrates an obvious rise in both the oxidation current–response and the reduction current–response when graphene is added to the system. This would suggest that the graphene is serving as a catalyst for this redox reaction in the liquid phase and allows for an increase in current–response. The inset in Fig. 3 shows the extent of the current–response for redox reaction (A) in the presence of increasing graphene concentrations.

### 3.3 Electrolyte preparation and fabrication and testing of DSSCs

Graphene dispersions in $CHCl_3$ were added to PMII at various concentrations ranging from 0.125 wt% to 3 wt%. The chloroform was allowed to evaporate from the IL over a period of 4–5 hours under Schlenk conditions. The photograph of ionic liquids with various concentrations of graphene is shown in Fig. 4. The graphene–ionic liquid composite electrolytes were then utilized to fabricate DSSCs.

The prepared graphene–ionic liquid composite electrolytes have been tested at a range of graphene concentrations. The presence of graphene in any concentration led to an increase in the efficiency of the DSSC when compared to the results obtained for PMII alone. PMMI showed an efficiency of 0.10% which agrees well with that found in the literature. The highest efficiency achieved for the composite electrolytes was 2.60% which was observed when an electrolyte was prepared at a concentration of 1.0 wt%. At graphene concentrations greater than 3 wt% the electrolyte begins to show behaviour similar to that of a quasi-solid based system. It is interesting to note that as the viscosity of these electrolytes increases they can still outperform the unmodified electrolyte. It was found that at graphene concentrations greater than 1.0 wt% excess amounts of graphene begin to impede the transfer of ions through the electrolyte and thus a drop in cell efficiency is noted (1.74% at 3 wt%). Analysis of the $J_{sc}$ obtained from these devices shows that upon addition of graphene an increase in the $J_{sc}$ can be observed, when compared to

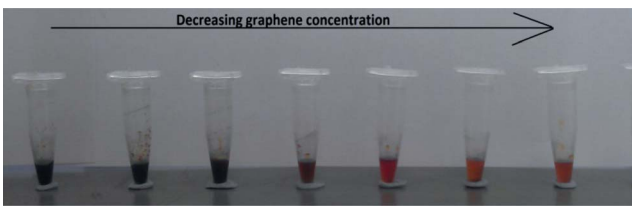


**Fig. 4** Photographic image of graphene–ionic liquid electrolytes showing increasing graphene concentration.

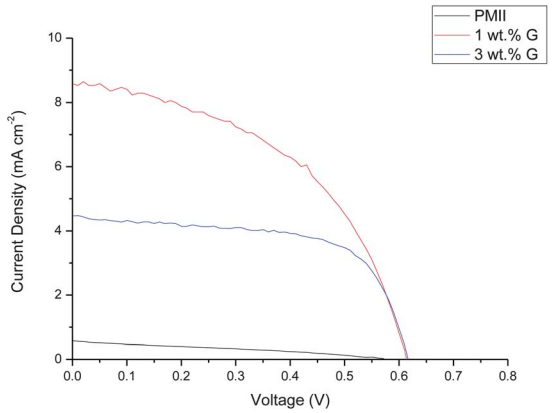


**Fig. 5** *I–V* curve obtained for PMII and graphene–IL composite electrolyte.

PMII. The increase in $J_{sc}$ can be attributed to the increased conductivity of the electrolyte. The $J_{sc}$ for the highest efficiency cell (1.0 wt% graphene added) was found to be 8.58 mA $cm^{-2}$. The $J_{sc}$ was observed to fall at graphene concentrations higher than 1 wt% and this can be attributed to the development of quasi-solid based systems at this concentration which impede the transport of ions through the electrolyte layer. Fig. 5 displays *I–V* curves showing a peak efficiency of 2.60% at 1000 W $m^{-2}$.

These results are rather different from our previous work on ionic liquids with a very high graphene content[17] and here we demonstrate that an increased efficiency can be achieved with much lower graphene concentrations. We believe that this is due to the electrolyte preparation and cell fabrication procedures. In the present work graphene is added to the IL in the liquid phase (dispersed in $CHCl_3$) rather than as a solid additive. In contrast to our previous work, where a very viscous gel-like electrolyte (with up to 40 wt% of graphene) was deposited on one of the electrodes in open air before the cell was sealed,[17] in our current work we use a liquid graphene–IL based electrolyte having a maximum 0.125–3.0 wt% of graphene and we employed a "closed cell" approach, where the cell was initially sealed and then the electrolyte was introduced into the cell under vacuum and then sealed with Surlyn. This approach enabled us to achieve much better efficiencies at low concentration of graphene (up to 2.6% at 1 wt% of graphene content) (Table 1).

**Table 1** Photovoltaic parameters obtained for DSSCs using graphene–ionic liquid composite electrolytes ($V_{oc}$ – open-circuit voltage; $J_{sc}$ – short-circuit current density; FF – fill factor and $\eta$ – efficiency)

| Graphene conc. (wt%) | $V_{oc}$ (V) | $J_{sc}$ (mA $cm^{-2}$) | FF | $\eta$ (%) |
|---|---|---|---|---|
| 0 | 0.57 | 0.59 | 0.31 | 0.10 |
| 0.125 | 0.52 | 2.41 | 0.25 | 0.31 |
| 0.25 | 0.55 | 4.11 | 0.28 | 0.64 |
| 0.50 | 0.60 | 3.85 | 0.44 | 1.03 |
| 1.0 | 0.61 | 8.58 | 0.49 | 2.60 |
| 3.0 | 0.61 | 4.47 | 0.63 | 1.74 |

## 4 Conclusions

In conclusion, we have demonstrated that the addition of small amounts (1.0 wt%) of graphene into ionic liquid based electrolytes results in a significant improvement of DSSC efficiency. The presence of graphene in the liquid electrolyte allows for a greater interaction between the IL and the graphene sheets. The increased level of interaction can facilitate a facile $\pi$–$\pi$ network to develop between the graphene and the IL. This enabled us to perform the preparation of highly uniform and stable dispersion of graphene in the IL, upon removal of chloroform. The resulting electrolyte can be considered as a composite liquid rather than an IL modified with solidifying agents.

We believe that the addition of graphene nanosheets also allows for an augmented electron pathway through the viscous IL electrolyte, owing primarily to the remarkable electronic properties of graphene. It is also expected that the graphene affords an EETS in the electrolyte, which facilitates the electrochemical reduction of $I_3^-$ in the electrolyte and thus lowers the diffusion length of the redox couple through the electrolyte. These results show that the addition of small amounts of graphene offers a viable route towards the preparation of ionic liquid composite electrolytes, which are more advanced than conventional solvent based systems.

## Acknowledgements

We thank IRCSET, EU FP7 (SMARTOP) programme and Solarprint Ltd for financial support.

## References

1 B. Oregan and M. Gratzel, *Nature*, 1991, **353**, 737–740.
2 M. Gratzel, *Inorg. Chem.*, 2005, **44**, 6841–6851.
3 M. Gratzel, *Nature*, 2001, **414**, 338–344.
4 M. K. Nazeeruddin, F. De Angelis, S. Fantacci, A. Selloni, G. Viscardi, P. Liska, S. Ito, B. Takeru and M. Grätzel, *J. Am. Chem. Soc.*, 2005, **127**, 16835–16847.
5 J. Wu, Z. Lan, J. Lin, M. Huang and P. Li, *J. Power Sources*, 2007, **173**, 585–591.
6 D. Wei, *Int. J. Mol. Sci.*, 2010, **11**, 1103–1113.
7 R. D. Rogers and K. R. Seddon, *Science*, 2003, **302**, 792–793.
8 J. Earle Martyn and R. Seddon Kenneth, in *Clean Solvents*, American Chemical Society, 2002, pp. 10–25.
9 T. Fukushima and T. Aida, *Chem.–Eur. J.*, 2007, **13**, 5048–5058.
10 M. Gorlov and L. Kloo, *Dalton Trans.*, 2008, 2655–2666.
11 P. Wang, S. M. Zakeeruddin, P. Comte, I. Exnar and M. Grätzel, *J. Am. Chem. Soc.*, 2003, **125**, 1166–1167.
12 H. Usui, H. Matsui, N. Tanabe and S. Yanagida, *J. Photochem. Photobiol., A*, 2004, **164**, 97–101.
13 E. Stathatos, P. Lianos, S. M. Zakeeruddin, P. Liska and M. Grätzel, *Chem. Mater.*, 2003, **15**, 1825–1829.
14 P. Wang, S. M. Zakeeruddin and M. Grätzel, *J. Fluorine Chem.*, 2004, **125**, 1241–1245.
15 P. Wang, S. M. Zakeeruddin, J. E. Moser, M. K. Nazeeruddin, T. Sekiguchi and M. Gratzel, *Nat. Mater.*, 2003, **2**, 402–407.

16 U. Bach, D. Lupo, P. Comte, J. E. Moser, F. Weissortel, J. Salbeck, H. Spreitzer and M. Gratzel, *Nature*, 1998, **395**, 583–585.
17 I. Ahmad, U. Khan and Y. K. Gun'ko, *J. Mater. Chem.*, 2011, **21**, 16990–16996.
18 A. K. Geim and K. S. Novoselov, *Nat. Mater.*, 2007, **6**, 183–191.
19 X. Wang, L. Zhi and K. Mullen, *Nano Lett.*, 2007, **8**, 323–327.
20 S. Bae, H. Kim, Y. Lee, X. F. Xu, J. S. Park, Y. Zheng, J. Balakrishnan, T. Lei, H. R. Kim, Y. I. Song, Y. J. Kim, K. S. Kim, B. Ozyilmaz, J. H. Ahn, B. H. Hong and S. Iijima, *Nat. Nanotechnol.*, 2010, **5**, 574–578.
21 G. Eda, G. Fanchini and M. Chhowalla, *Nat. Nanotechnol.*, 2008, **3**, 270–274.
22 S. Stankovich, D. A. Dikin, G. H. B. Dommett, K. M. Kohlhaas, E. J. Zimney, E. A. Stach, R. D. Piner, S. T. Nguyen and R. S. Ruoff, *Nature*, 2006, **442**, 282–286.
23 T. Ramanathan, A. A. Abdala, S. Stankovich, D. A. Dikin, M. Herrera Alonso, R. D. Piner, D. H. Adamson, H. C. Schniepp, X. Chen, R. S. Ruoff, S. T. Nguyen, I. A. Aksay, R. K. Prud'Homme and L. C. Brinson, *Nat. Nanotechnol.*, 2008, **3**, 327–331.
24 T. Kuilla, S. Bhadra, D. Yao, N. H. Kim, S. Bose and J. H. Lee, *Prog. Polym. Sci.*, 2010, **35**, 1350–1375.
25 S. Villar-Rodil, J. I. Paredes, A. Martinez-Alonso and J. M. D. Tascon, *J. Mater. Chem.*, 2009, **19**, 3591–3593.
26 L. J. Brennan, M. T. Byrne, M. Bari and Y. K. Gun'ko, *Adv. Energy Mater.*, 2011, **1**, 472–485.
27 W. Hong, Y. Xu, G. Lu, C. Li and G. Shi, *Electrochem. Commun.*, 2008, **10**, 1555–1558.
28 X. Wang, L. Zhi, N. Tsao, Ž. Tomović, J. Li and K. Müllen, *Angew. Chem.*, 2008, **120**, 3032–3034.
29 T. Fukushima, A. Kosaka, Y. Ishimura, T. Yamamoto, T. Takigawa, N. Ishii and T. Aida, *Science*, 2003, **300**, 2072–2074.
30 P. Hasin, M. A. Alpuche-Aviles and Y. Wu, *J. Phys. Chem. C*, 2010, **114**, 15857–15861.
31 S. Ito, P. Chen, P. Comte, M. K. Nazeeruddin, P. Liska, P. Péchy and M. Grätzel, *Progr. Photovolt.: Res. Appl.*, 2007, **15**, 603–612.
32 A. O'Neill, U. Khan, P. N. Nirmalraj, J. Boland and J. N. Coleman, *J. Phys. Chem. C*, 2011, **115**, 5422–5428.
33 A. C. Ferrari, J. C. Meyer, V. Scardaci, C. Casiraghi, M. Lazzeri, F. Mauri, S. Piscanec, D. Jiang, K. S. Novoselov, S. Roth and A. K. Geim, *Phys. Rev. Lett.*, 2006, **97**, 187401.
34 M. S. Dresselhaus, A. Jorio and R. Saito, *Annu. Rev. Condens. Matter Phys.*, 2010, **1**, 89–108.
35 Y. Hernandez, V. Nicolosi, M. Lotya, F. M. Blighe, Z. Sun, S. De, I. T. McGovern, B. Holland, M. Byrne, Y. K. Gun'Ko, J. J. Boland, P. Niraj, G. Duesberg, S. Krishnamurthy, R. Goodhue, J. Hutchison, V. Scardaci, A. C. Ferrari and J. N. Coleman, *Nat. Nanotechnol.*, 2008, **3**, 563–568.

 